J Mater Sci: Mater Electron (2016) 27:6122–6127
DOI 10.1007/s10854-016-4538-x

Sulfuric acid vapor treatment for enhancing the thermoelectric properties of PEDOT:PSS thin-films

Jaeyun Kim[1] · Jae Gyu Jang[2] · Jong-In Hong[2] · Sung Hyun Kim[2] · Jeonghun Kwak[1]

Received: 30 December 2015 / Accepted: 14 February 2016 / Published online: 20 February 2016

Abstract We introduce a sulfuric acid vapor treatment method to enhance the thermoelectric (TE) performance of poly(3,4-ethylenedioxythiophene):poly(styrenesulfonate) (PEDOT:PSS) thin-films. The H_2SO_4 vapor treatment brought about the reduction of Coulomb interaction between PEDOT and PSS chains and structural rearrangement of PEDOT:PSS as expanded coil-like nanostructure. We studied the effects of the H_2SO_4 vapor treatment on the electrical conductivity and TE properties of PEDOT:PSS thin-films at various treatment temperatures. By the H_2SO_4 vapor treatment at 140 °C, both electrical conductivity and Seebeck coefficient of the PEDOT:PSS thin-film were improved from 1.1 to 1167 S/cm, and from 7.3 to 12.1 μV/K, respectively. At this condition, the maximum power factor of 17.0 $\mu W/mK^2$ was obtained, which is higher than that of the pristine PEDOT:PSS film (0.006 $\mu W/mK^2$) by the factor of 2833. Because the H_2SO_4 vapor treatment method introduced here has advantages in the large-area process and the film uniformity, we believe that the method can be applicable to various organic electronic devices using PEDOT:PSS as well as TE devices.

1 Introduction

Recently, the development of the energy harvesting technologies such as solar cells and aero-generators has attracted a great deal of attention. These nature-oriented technologies are free to the environmental pollution and the exhaustion of resources. However, a lot of constraints obstruct the widespread use of them, such as high cost, colossal size, and qualified environmental condition to construct. On the other hand, thermoelectric (TE) devices, which convert waste heat to electricity, are unrestricted to those conditions; they can be attached to any surfaces dissipating heat, with the sizes from small to large. In particular, thin-film TE devices based on polymers, organic materials, and organic–inorganic composites expands the application field by the virtues of easy process, low cost, and high flexibility in their form factor [1–3]. Although the performance of thin-film TE devices is inferior compared to that of typical TE devices using inorganic compounds such as Bi_2Te_3 and PbTe [4, 5], years of multilateral efforts on the development/understanding of materials and device physics bring about a rapidly advancement of thin-film TE properties [1–3].

Among various organic/polymer materials, poly(3,4-ethylenedioxythiophene):poly(styrenesulfonate) (PEDOT:PSS) has superb electrical conductivity (σ) over 1000 S/cm. Owing to the high electrical conductivity, thin-film TE devices using PEDOT:PSS exhibit a good power factor (PF) or a thermoelectric figure of merit (ZT), which are defined as $PF = S^2\sigma$ and $ZT = S^2\sigma T/\kappa$, respectively,

Jaeyun Kim and Jae Gyu Jang have contributed equally to this article.

✉ Sung Hyun Kim
shkim75@snu.ac.kr

✉ Jeonghun Kwak
jkwak82@uos.ac.kr

[1] School of Electrical and Computer Engineering, The University of Seoul, Seoul 02504, Korea

[2] Department of Chemistry, Seoul National University, Seoul 08826, Korea

where S, T, and κ are the Seebeck coefficient, absolute temperature, and thermal conductivity, respectively. Moreover, the TE properties of PEDOT:PSS thin-films can be improved by increasing the electrical conductivity and/or the Seebeck coefficient. As shown in the definition of ZT, it is certain that increasing both electrical conductivity and Seebeck coefficient enables us to obtain the highest ZT. However, the two parameters are in inversely proportional to each other. In other words, higher electrical conductivity is generally obtainable by higher carrier density in semiconductors. Higher carrier density means higher thermal conductivity, which tends to decrease the Seebeck coefficient. Due to the relation, optimization between the electrical conductivity and Seebeck coefficient is one of the important factors to enhance the TE performance. The electrical conductivity of PEDOT:PSS can be increased by adding polar solvents (e.g. ethylene glycol or dimethyl sulfoxide) [6–8] and replacing PSS with efficient counterions such as tosylate and bis(trifluoromethylsulfonyl)imide [9, 10]. The highest electrical conductivity (more than 3000 S/cm) of a PEDOT:PSS thin-film was reported by Xia et al. [11] by dropping H_2SO_4 solution on a PEDOT:PSS film. To increase the Seebeck coefficient of PEDOT:PSS, a few methods, for instance, fabricating PEDOT:PSS based composite films [12–16], post-treatments [17–19], and controlling the redox state of the films [8, 9, 20–22], have been introduced. Through the research, the ZT of PEDOT:PSS have been increased from 10^{-3} (pristine PEDOT:PSS) to 10^{-2}–10^{-1} (depending on additive/treatment condition) [6–10, 12–21]. Meanwhile, a few groups recently reported the improved performance of PEDOT-based TE devices with droplets of H_2SO_4 [23, 24]. However, dropping acidic vapor onto the solid PEDOT:PSS films makes the surface morphology rough. Also, inhomogeneity of both film properties and their device performance is unavoidable.

Here, we introduce a novel post-treatment method to increase both electrical conductivity and TE properties of PEDOT:PSS thin-films, which is the H_2SO_4 vapor treatment. The H_2SO_4 vapor changed PEDOT:PSS to the expanded coil-like nanostructure by the reorientation of PEDOT and PSS chains similar with the H_2SO_4 droplet treatment. Moreover, the vapor-treated film showed much smoother surface morphology and higher uniformity than the droplet treatment. As a result of the vapor treatment, the electrical conductivity was enhanced to 1167 S/cm after the H_2SO_4 vapor treatment at 140 °C. At the same conditions, the Seebeck coefficient was also improved to 16.5 μV/K. Owing to the simultaneous improvement of the electrical conductivity and Seebeck coefficient, a high PF of 17.0 $\mu W/mK^2$ was obtained, which is over three orders of magnitude higher than that of the pristine PEDOT:PSS thin-film (0.006 $\mu W/mK^2$). The effect of the annealing temperature on the TE performance of the H_2SO_4-treated PEDOT:PSS films were investigated in this work.

2 Experimental section

The PEDOT:PSS solution (Clevios PH 1000) with the concentration of 1.3 wt% dispersed in water was purchased from H. C. Starck GmbH. The weight ratio of PEDOT to PSS was 2.5. Sulfuric acid (95 %) was obtained from Samchun Chemical.

For the film preparation, glass substrates were cleaned with deionized water and isopropyl alcohol in a sonication bath, followed by drying in a vacuum oven for 12 h. Before coating the PEDOT:PSS, the substrates were exposed to UV-ozone for 5 min. The PEDOT:PSS aqueous solution filtered through a 0.45 μm syringe filter was spin coated onto the glass substrates at a rate of 2300 rpm for 40 s. Then, it was pre-baked at 120 °C for 2 min. For the H_2SO_4 vapor treatment, we put the samples and a 10 M H_2SO_4 solution (2 ml) inside the pre-heated vacuum chamber, and kept a low vacuum state ($\sim 10^{-2}$ Pa) to maintain the H_2SO_4 vapor atmosphere for 15 min which is the optimum treatment time. In other words, the electrical conductivity was saturated after 15 min. Here, various annealing temperature conditions (130–160 °C) were examined, because the annealing temperature is one of the most critical factors for the structural rearrangement and crystallization of the PEDOT:PSS films [25, 26]. In order to remove the residual H_2SO_4, as-treated PEDOT:PSS films were annealed at 150 °C for 10 min. To fabricate the TE devices, Au electrodes of 100 nm were thermally evaporated on the PEDOT:PSS film through a shadow mask under a base pressure of $<10^{-4}$ Pa.

The thickness (t) and the morphology of the films were measured with an alpha-step profilometer and atomic force microscopy (AFM, Veeco, NanoScope IV), respectively. The sheet resistance (R_S) was measured with a four-point probe system, which was used to calculate the electrical conductivity (σ) with the equation $\sigma = 1/R_S \times t$. The thermovoltage generated by the temperature gradient (ΔV) in the film was measured with a digital multimeter (Agilent 3458A) while the temperature difference (ΔT) was monitored by two type-K thermocouples connected to each electrode. All instruments were connected to a computer and controlled with LabView.

3 Results and discussion

Figure 1a shows the thickness of the pristine and H_2SO_4 vapor treated PEDOT:PSS thin-film as a function of the annealing temperature. The thickness of the pristine sample

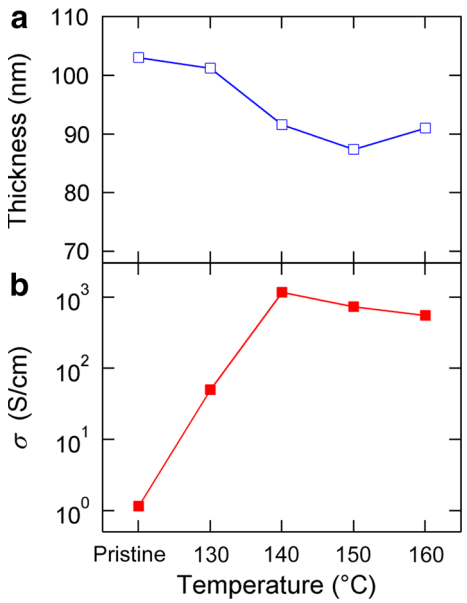

Fig. 1 **a** The thickness and **b** electrical conductivity of the H_2SO_4-treated PEDOT:PSS thin-films depending on the annealing temperature

was 103 nm, and the thicknesses of the samples were reduced after the H_2SO_4 vapor treatment, which is analogous to the previous report [11]. In particular, we found that the thickness was decreased more and more as the annealing temperature was increased from 130 to 150 °C. It is attributed to two reasons: a higher temperature promotes (1) the selective removal of PSS from PEDOT by the reduction of Coulomb interaction between them and (2) the rearrangement and crystallization of both PEDOT and PSS.

Figure 1b plots the electrical conductivity of the pristine and H_2SO_4 vapor-treated PEDOT:PSS thin-films as a function of the vapor annealing temperature. The electrical conductivity of the pristine film was approximately 1.1 S/cm. It is well-known that the electrical conductivity is limited by the insulating PSS-rich shells surrounding the conducting PEDOT-rich grains [27, 28]. PEDOT:PSS consists of the conducting (positive charged) PEDOT chains and the insulating (negative charged) PSS counterions for chemical stability, which make it possible to be dispersed in water due to the Coulomb interaction. However, by the detachment of PSS as mentioned above during H_2SO_4 vapor treatment, the values were drastically increased. Among the samples, the PEDOT:PSS thin-film treated at 140 °C showed the maximum electrical conductivity of 1167 S/cm, which is three orders of magnitude higher than that of the pristine thin-film.

It has been known that the nature of the hopping conduction mechanism of the conjugated polymer relies mainly on the doping state and molecular structure. Thus, the electrical conductivity of the polymers can be manipulated by controlling the degree of oxidation, molecular orientation, and so on. For this purpose, we adopted the H_2SO_4 vapor treatment method to PEDOT:PSS films. A strong acid solvent, H_2SO_4, capable of being both a proton donor and a proton acceptor can undergo autoprotolysis [29] according to the general process:

$$H_2SO_4 \leftrightarrow H^+ + HSO_4^- \quad (1)$$

Therefore, when PEDOT:PSS is treated with H_2SO_4, the proton donors associate with PSS^- as follows,

$$PSS^- + H^+ \leftrightarrow PSSH \quad (2)$$

which reduces the Coulomb interaction between PEDOT and PSS chains. Consequently, the addition of the H_2SO_4 molecules into the PEDOT:PSS film during the annealing process induces the phase separation between PEDOT and PSS chains, which can facilitate the structural reorientation and enhance the π–π interaction of PEDOT chains. After all, the enhanced π–π stacking between PEDOT moieties gives rise to change the morphology as expanded coil-like nanostructures [30–32]. As a result, the energy barrier for inter- and intra- chain of PEDOT was lowered [33], leading to the improvement of the conductivity of PEDOT:PSS by H_2SO_4 vapor treatment at 140 °C.

We have also measured and compared the film morphology of the PEDOT:PSS films before and after the H_2SO_4 treatment at 140 °C by AFM. The topographic and phase images in Fig. 2a, b represent the surface of the pristine PEDOT:PSS film, which is similar with general polymer thin-films due to the homogeneously distributed polymer chains of PEDOT and PSS. On the contrary, in the H_2SO_4-treated PEDOT:PSS film, the size of PEDOT domains was increased and thus the boundaries were reduced as shown in Fig. 2c, d, induced by the aggregation of PEDOT chains. The phase images display the drastic difference between two films more clearly. Also, the H_2SO_4-treated PEDOT:PSS film has a smoother surface than the pristine PEDOT:PSS film, i.e., the root mean square (RMS) roughness of the PEDOT:PSS films with and without the H_2SO_4 treatment were 0.82 and 1.27, respectively. The results are considered to be a good evidence for the reorientation of PEDOT and PSS chains during the H_2SO_4 vapor treatment. Furthermore, the result is meaningful in the viewpoint of the improved surface morphology for thin-film electronic devices. Previous report using the drops of H_2SO_4 solution on a PEDOT:PSS film showed that the RMS roughness was increased by 1.8 times (1.63–2.95 nm) after the treatment due to the drastic changes in the film [11]. However, the vapor treatment method presented here decreased the roughness. We attribute the result to the merits of the H_2SO_4 vapors treatment as follows: (1) the vapor can penetrate more slowly, deeply, and homogeneously into the polymer chains than the

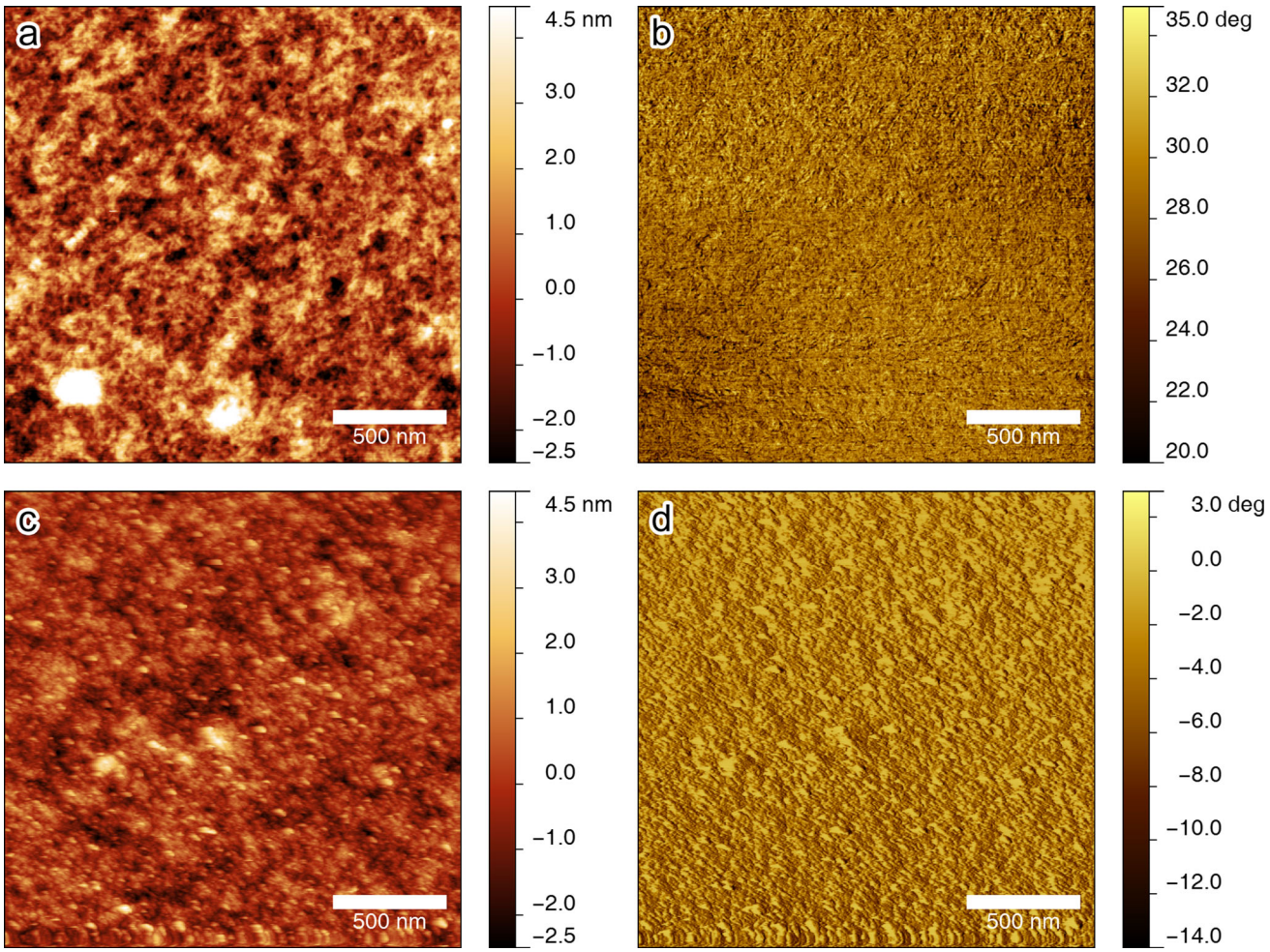

Fig. 2 The AFM topographic images (**a**, **c**) and phase images (**b**, **d**) of the PEDOT:PSS thin-films before (**a**, **b**) and after (**c**, **d**) the H_2SO_4 vapor treatment at 140 °C

solution drop treatment, resulting in a uniform chemical reaction within the whole films; (2) because the interaction of H_2SO_4 and PEDOT:PSS and the annealing of PEDOT:PSS films proceed simultaneously, the reorientation of the film might be much activated. As a result, both PEDOT and PSS chains can construct a smooth and well-ordered film. Therefore, proper aggregation of PEDOT chains could control the conjugated π-electrons delocalization over the whole chain, enhancing the improvement conductive path of in terms of an electrical percolation. It also explains the superior electrical properties than the other vapor-treated PEDOT:PSS films [18, 19].

Using the PEDOT:PSS thin-films by this process, we fabricated TE devices and characterized their TE properties. Figure 3a shows the schematic illustration of the TE device structure and the measurement system. In detail, the device was placed over two Peltier modules of which each temperature was controlled by a multi-channel direct current source. The temperature difference between two Peltier modules brings about the thermovoltage across the hot and cool electrodes. From the measured data, we calculated the Seebeck coefficient of the films using the equation $S = \Delta V/\Delta T$. Figure 3b shows the Seebeck coefficient and PF of the prepared PEDOT:PSS thin-films depending on the annealing temperature during the H_2SO_4 vapor treatment. The Seebeck coefficient of the non-treated film was 7.3 μV/K. The value was increased up to 16.5 μV/K with the H_2SO_4 vapor treatment at 130 °C, which is much higher than the films treated with H_2SO_4 droplets [24]. Then the value was slightly reduced as the temperature increased. The PF was calculated as 0.006 $\mu W/mK^2$ in the pristine film. At 130 °C, the PF was slightly increased to 1.4 $\mu W/mK^2$ due to the low electrical conductivity, even though the Seebeck coefficient is the highest at this temperature. The maximum PF of 17.0 $\mu W/mK^2$ was obtained at 140 °C with the Seebeck coefficient of 12.1 μV/K, which is the temperature for the highest electrical conductivity. In other words, the PF was

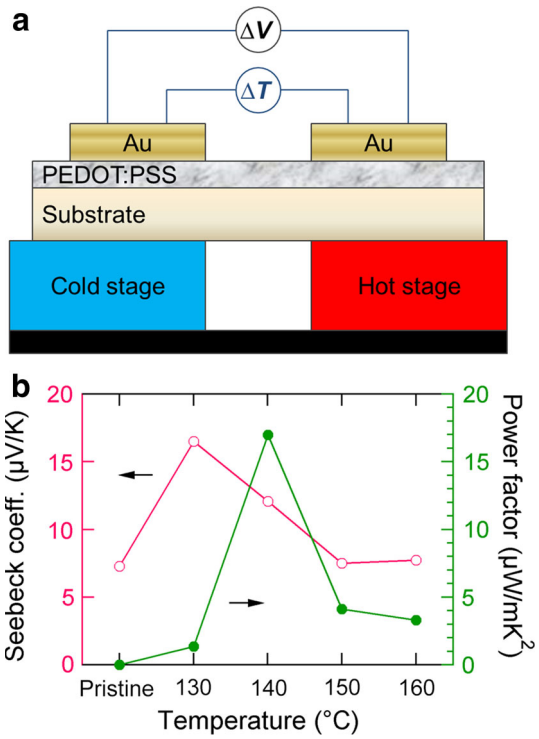

Fig. 3 **a** The schematic diagram of the thermoelectric device and the measurement setup. **b** The Seebeck coefficient (*open circle*) and power factor (*closed circle*) of the PEDOT:PSS thin-films depending on the annealing temperature during the H_2SO_4 vapor treatment

enhanced by >3 orders of magnitude via the H_2SO_4 vapor treatment. This result also shows that the optimization between the electrical conductivity and Seebeck coefficient is a meaningful study to obtain high TE properties.

4 Conclusion

In conclusion, we introduced the H_2SO_4 vapor treatment method to enhance both electrical conductivity and TE properties of PEDOT:PSS thin-films. With changing the treatment temperature, we investigated the electrical conductivity and Seebeck coefficient of the films and found the optimum condition to achieve the performance of PEDOT:PSS-based TE devices. The thin-film treated with H_2SO_4 vapor at 140 °C exhibited a high PF which was over three orders of magnitude higher than that of the non-treated sample. The enhancement was attributed to the improvement in both of the electrical conductivity and Seebeck coefficient owing to the formation of highly ordered and densely packed PEDOT:PSS as an expanded coil-like nanostructure by strong acidic H_2SO_4. Also, the vapor treatment to PEDOT:PSS film exhibited smooth and uniform morphology. Therefore, we believe that this method introduced here is helpful not only for polymer-based TE devices, but also for the optoelectronic devices using polymer electrodes.

Acknowledgments This research was supported by Basic Science Research Program through the National Research Foundation of Korea (NRF) funded by the Ministry of Education (NRF-2014R1A1A2055322 and NRF-2015R1D1A1A01060185).

References

1. R. Yue, J. Xu, Synth. Met. **162**, 912 (2012)
2. M. Culebras, C.M. Gómez, A. Cantarero, Materials **7**, 6701 (2014)
3. M. He, F. Qiu, Z. Lin, Energy Environ. Sci. **6**, 1352 (2013)
4. B. Poudel, Q. Hao, Y. Ma, Y. Lan, A. Minnich, B. Yu, X. Yan, D. Wang, A. Muto, D. Vashaee, X. Chen, J. Liu, M.S. Dresselhaus, G. Chen, Z. Ren, Science **320**, 634 (2008)
5. Y. Pei, X. Shi, A. LaLonde, H. Wang, L. Chen, G.J. Snyder, Nature **473**, 66 (2011)
6. G.-H. Kim, L. Shao, K. Zhang, K.P. Pipe, Nat. Mater. **12**, 719 (2013)
7. K. Sun, S. Zhang, P. Li, Y. Xia, X. Zhang, D. Du, F.H. Isikgor, J. Ouyang, J. Mater. Sci. Mater. Electron. **26**, 4438 (2015)
8. E. Yang, J. Kim, B.J. Jung, J. Kwak, J. Mater. Sci. Mater. Electron. **26**, 2838 (2015)
9. O. Bubnova, Z.U. Khan, A. Malti, S. Braun, M. Fahlman, M. Berggren, X. Crispin, Nat. Mater. **10**, 429 (2011)
10. M. Culebras, C.M. Gómez, A. Cantarero, J. Mater. Chem. A **2**, 10109 (2014)
11. Y. Xia, K. Sun, J. Ouyang, Adv. Mater. **24**, 2436 (2012)
12. D. Kim, Y. Kim, K. Choi, J.C. Grunlan, C. Yu, ACS Nano **1**, 513 (2010)
13. K. Xu, G. Chen, D. Qiu, J. Mater. Chem. A **1**, 12395 (2013)
14. Q. Jiang, C. Liu, J. Xu, B. Lu, H. Song, H. Shi, Y. Yao, L. Zhang, J. Polym. Sci. Part B Polym. Phys. **52**, 737 (2014)
15. Z. Zhang, G. Chen, H. Wang, X. Li, Chem. Asian J. **10**, 149 (2015)
16. Q. Jiang, C. Liu, H. Song, J. Xu, D. Mo, H. Shi, Z. Wang, F. Jiang, B. Lu, Z. Zhu, Int. J. Electrochem. Sci. **9**, 7540 (2014)
17. N. Massonnet, A. Carella, O. Jaudouin, P. Rannou, G. Laval, C. Celle, J.-P. Simonato, J. Mater. Chem. C **2**, 1278 (2014)
18. L. Zhang, H. Deng, S. Liu, Q. Zhang, F. Chen, Q. Fu, RSC Adv. **5**, 105592 (2015)
19. Q. Jiang, C. Liu, H. Song, H. Shi, Y. Yao, J. Xu, G. Zhang, B. Lu, J. Mater. Sci. Mater. Electron. **24**, 4240 (2013)
20. J. Luo, D. Billep, T. Waechtler, T. Otto, M. Toader, O. Gordan, E. Sheremet, J. Martin, M. Hietschold, D.R.T. Zahn, T. Gessner, J. Mater. Chem. A **1**, 7576 (2013)
21. T. Park, C. Park, B. Kim, H. Shin, E. Kim, Energy Environ. Sci. **6**, 788 (2013)
22. J. Wang, K. Cai, S. Shen, Org. Electron. **17**, 151 (2015)
23. J. Wang, K. Cai, S. Shen, Org. Electron. **15**, 3087 (2014)
24. S. van Reenen, M. Scheepers, K. van de Ruit, D. Bollen, M. Kemerink, Org. Electron. **15**, 3710 (2014)
25. O.P. Dimitriev, D.A. Grinko, Y.V. Noskov, N.A. Ogurtsov, A.A. Pud, Synth. Met. **159**, 2237 (2009)
26. Y. Kim, A.M. Ballantyne, J. Nelson, D.D.C. Bradley, Org. Electron. **10**, 205 (2009)
27. U. Lang, E. Müller, N. Naujoks, J. Dual, Adv. Funct. Mater. **19**, 1215 (2009)
28. J. Huang, P.F. Miller, J.S. Wilson, A.J. de Mello, J.C. de Mello, D.D.C. Bradley, Adv. Funct. Mater. **15**, 290 (2005)

29. N.N. Greenwood, A. Earnshaw, *Chemistry of the Elements* (Butterworth-Heinemann, Oxford, 1997)
30. N. Kim, B.H. Lee, D. Choi, G. Kim, H. Kim, J.-R. Kim, J. Lee, Y.H. Kahng, K. Lee, Phys. Rev. Lett. **109**, 106405 (2012)
31. E.-G. Kim, J.-L. Brédas, J. Am. Chem. Soc. **130**, 16880 (2008)
32. X. Guo, N. Zhou, S.J. Lou, J.W. Hennek, R.P. Ortiz, M.R. Butler, P.-L.T. Boudreault, J. Strzalka, P.-O. Morin, M. Leclerc, J.T.L. Navarrete, M.A. Ratner, L.X. Chen, R.P.H. Chang, A. Facchetti, T.J. Marks, J. Am. Chem. Soc. **134**, 18427 (2012)
33. S.B. Darling, J. Phys. Chem. B **112**, 8891 (2008)